

# Magnetic properties of $Y_2Fe_{17-x}Ga_x$ and $Sm_2Fe_{17-x}Ga_x$ compounds

FUMIO MARUYAMA

177-11, Shimadachi, Matsumoto, 390-0852, Japan

E-mail: fmaruya@shinshu-u.ac.jp

Published online: 5 October 2005

The magnetic properties of  $Y_2Fe_{17-x}Ga_x$  and  $Sm_2Fe_{17-x}Ga_x$  for  $3 \leq x \leq 7$  have been investigated using the  $^{57}Fe$  Mössbauer spectroscopy at room temperature. These compounds have the rhombohedral  $Th_2Zn_{17}$  structure. X-ray diffraction analyses of aligned powders show that the easy direction of magnetization is parallel to the c-axis in  $Y_2Fe_{10}Ga_7$  and  $Sm_2Fe_{14}Ga_3$  and is perpendicular to the c-axis in  $Y_2Fe_{14}Ga_3$ ,  $Y_2Fe_{12}Ga_5$ ,  $Sm_2Fe_{12}Ga_5$  and  $Sm_2Fe_{10}Ga_7$ . Mössbauer studies indicate that all the samples studied are ferromagnetically ordered. The  $^{57}Fe$  hyperfine field decreases with increasing Ga content. This decrease results from the decreased magnetic exchange interactions resulting from Ga substitution. The average isomer shift,  $\delta$ , for  $Y_2Fe_{17-x}Ga_x$  and  $Sm_2Fe_{17-x}Ga_x$  at room temperature is positive and the magnitude of  $\delta$  increases with increasing Ga content.

© 2005 Springer Science + Business Media, Inc.

## 1. Introduction

The  $R_2Fe_{17}$  compounds are not suitable for permanent magnet materials, because the magnetic anisotropy is planar. The substitution of nonmagnetic atoms, Ga, Al and Si, for Fe in  $R_2Fe_{17}$  has a profound influence on the magnetic properties, especially on determining the easy magnetization direction [1–3].

For  $R_2Fe_{17-x}Ga_x$  ( $R = Y, Sm, Gd, Tb, Dy, Ho, Er$  and  $Tm$ ), the Curie temperature,  $T_C$ , first strongly increase with increasing Ga content in spite of decreasing the value of  $\mu_{Fe}$  and go through a maximum value, then decrease with  $x$  [4–9]. Moreover, it is surprising that the values of  $T_C$  increase again at a higher Ga concentration ( $x > 6$ ) for  $R_2Fe_{17-x}Ga_x$  ( $R = Ho$  and  $Tm$ ) and ( $x > 7$ ) for  $Y_2Fe_{17-x}Ga_x$ .

By Ga substitution for Fe, the magnetic anisotropy changes from planar to axial at room temperature [1]. An uniaxial anisotropy at room temperature in  $R_2Fe_{17-x}Ga_x$  is shown with high Ga concentration, at  $x = 6, 7, 8$  for  $R = Tb$  and  $Dy$ ,  $x = 7, 8$  for  $R = Y, Gd$  and  $Tm$  and  $x = 8$  for  $R = Er$ . Whereas for  $R = Sm$ , the magnetic anisotropy is planar at  $x = 0, 7, 8$  and axial at  $x = 3, 4$ . Hence, the magnetic properties of  $R_2Fe_{17-x}Ga_x$  are very interesting. In our previous study [10], we calculated the molecular field coefficients,  $n_{FeFe}$  and  $n_{RFe}$  ( $R = Sm, Gd, Tb, Ho$  and  $Tm$ ), for  $R_2Fe_{17-x}Ga_x$  and the values of  $n_{FeFe}$  and  $n_{SmFe}$  for  $R_2Fe_{17-x}T_x$  ( $T = Al$  and  $Si$ ) using the experimental values of  $T_C$ . The values of  $n_{FeFe}$  increase in spite of the decrease of  $\mu_{Fe}$  for  $0 \leq x \leq 5$  in  $Y_2Fe_{17-x}Ga_x$ . The values of  $n_{SmFe}$  have large values when the magnetic anisotropy is axial. For  $6 \leq x \leq 8$ , the values of  $n_{FeFe}$ ,  $n_{HoFe}$  and  $n_{TmFe}$  increase strongly, which is related to the change of the easy magnetization direction.

0022-2461 © 2005 Springer Science + Business Media, Inc.  
DOI: 10.1007/s10853-005-1600-0

In this paper, we report the results of Mössbauer experiments for  $Y_2Fe_{17-x}Ga_x$  and  $Sm_2Fe_{17-x}Ga_x$  and study the effect of Ga on the magnetic properties.

## 2. Experimental

The samples were prepared in an induction furnace in a purified argon atmosphere. The purities were 99.9% for Fe, Y and Sm and 99.999% for Ga. Ingots sealed in evacuated quartz tubes were annealed for one week at 950°C. Structural analysis was carried out using X-ray diffraction with  $Fe-K\alpha$  radiation at room temperature. To determine the easy direction of magnetization X-ray diffraction analyses of aligned powders were performed. The specimens were ground to a fine powder and fixed in a magnetic field by a permanent magnet for orientation in the easy magnetization direction of the particle. When the particle has an easy basal plane anisotropy, as confirmed by the reflected X-ray intensity from the plane perpendicular to the applied field, the (hk0) intensity increases strongly and the (00l) intensity diminishes. When the particle has an easy c-axis anisotropy, the (00l) intensity increases strongly and the (hk0) intensity diminishes. The  $^{57}Fe$  Mössbauer spectra were measured with a conventional constant-acceleration spectrometer at room temperature. The  $\gamma$ -ray source was  $^{57}Co$  in a Rh matrix. Calibration was made by using the spectrum of  $\alpha-Fe_2O_3$  at room temperature.

## 3. Results and discussion

A single rhombohedral  $Th_2Zn_{17}$  type phase was found for  $x = 3$  and 7 in  $Y_2Fe_{17-x}Ga_x$ , but for  $x = 5$  the small amount of  $\alpha-Fe$  phase is also present. The

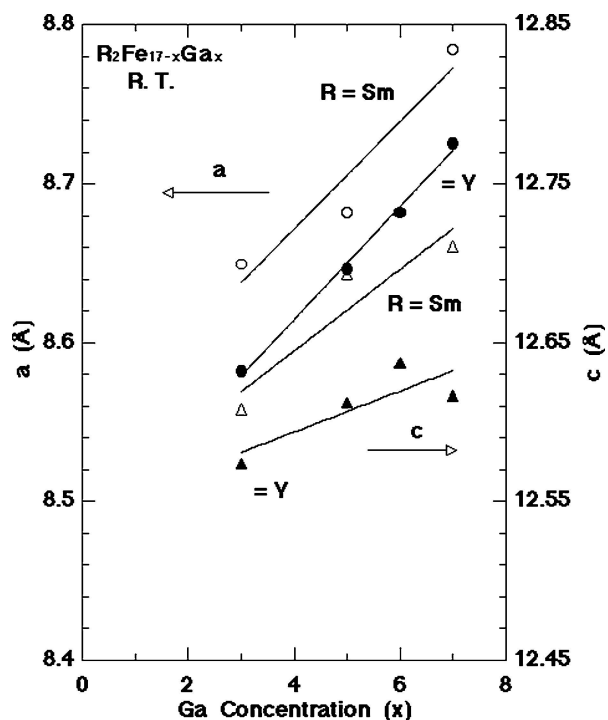


Figure 1 The dependence of the lattice constant  $a$  and  $c$  on the Ga concentration for  $Y_2Fe_{17-x}Ga_x$  and  $Sm_2Fe_{17-x}Ga_x$ .

rhombohedral  $Th_2Zn_{17}$  type phase is the main phase present with the  $\alpha$ -Fe phase for  $3 \leq x \leq 7$  in  $Sm_2Fe_{17-x}Ga_x$ . The concentration dependences of the lattice constants  $a$  and  $c$  at room temperature for  $Y_2Fe_{17-x}Ga_x$  and  $Sm_2Fe_{17-x}Ga_x$  are shown in Fig. 1. The lattice constants,  $a$  and  $c$ , increased with increasing Ga content. The increase in  $a$  is larger than that in  $c$ .

The concentration dependences of the ratio  $c/a$  and the unit-cell volume  $V$  at room temperature for  $Y_2Fe_{17-x}Ga_x$  and  $Sm_2Fe_{17-x}Ga_x$  are shown in Fig. 2.

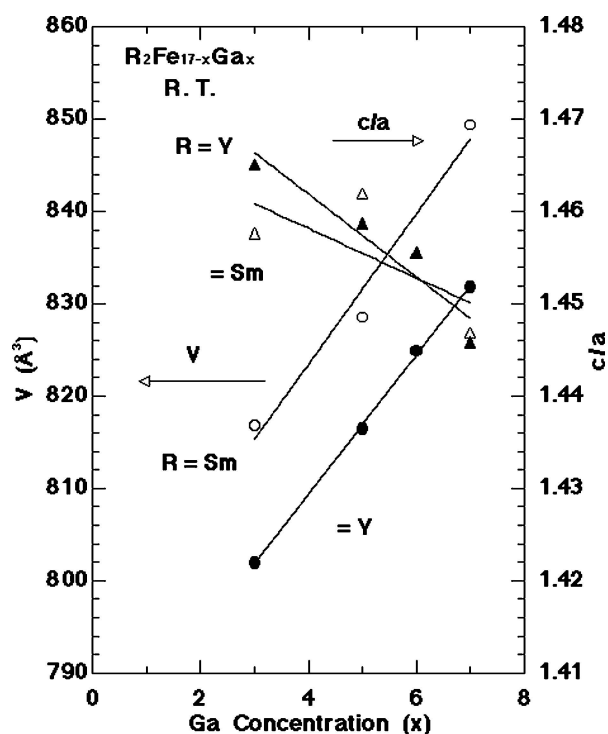


Figure 2 The dependence of the unit cell volume,  $V$ , and  $c/a$  on the Ga concentration for  $Y_2Fe_{17-x}Ga_x$  and  $Sm_2Fe_{17-x}Ga_x$ .

The values of  $c/a$  decreased and those of  $V$  increased with increasing Ga content.

X-ray diffraction analyses of aligned powders were performed to determine the easy direction of magnetization. In  $Y_2Fe_{10}Ga_7$  and  $Sm_2Fe_{14}Ga_3$ , the reflected X-ray intensity (006) is strengthened, so the easy direction of magnetization is parallel to the  $c$ -axis. In  $Y_2Fe_{14}Ga_3$ ,  $Y_2Fe_{12}Ga_5$ ,  $Sm_2Fe_{12}Ga_5$  and  $Sm_2Fe_{10}Ga_7$ , the reflected X-ray intensities (300) and (220) are strengthened, hence the easy direction of magnetization is perpendicular to the  $c$  axis.

For  $Y_2Fe_{10}Ga_7$ , the Ga atoms occupy at the 6c, 9d, 18f and 18h sites with the occupation ratio, 0.80, 0, 0.65 and 0.25, respectively [11]. For  $Y_2Fe_{12}Ga_5$ , the Ga atoms occupy at the 6c, 9d, 18f and 18h sites with the occupancy 0, 0, 0.40 and 0.42, respectively [11].

The dependence of  $T_C$  on the Ga concentration for  $Y_2Fe_{17-x}Ga_x$  and  $Sm_2Fe_{17-x}Ga_x$  taken from Ref. [4] and [5], respectively is shown in Fig. 3. The values of  $T_C$  first increase with increasing Ga content and decrease, but it is surprising that those of  $T_C$  increase again at a higher Ga concentration ( $x > 7$ ) for  $Y_2Fe_{17-x}Ga_x$ . The dependence of the value of  $\mu_{Fe}$  on the Ga concentration at 15 K for  $Y_2Fe_{17-x}Ga_x$  taken from Ref. [4], is also shown in Fig. 3. The values of  $\mu_{Fe}$  decreased with increasing Ga content.

The Mössbauer spectra and their fitted curves for  $Y_2Fe_{17-x}Ga_x$  and  $Sm_2Fe_{17-x}Ga_x$  at room temperature are shown in Figs 4 and 5, respectively. The  $^{57}Fe$  Mössbauer spectra show hyperfine split sextets in  $Y_2Fe_{17-x}Ga_x$  and  $Sm_2Fe_{17-x}Ga_x$  revealing that the samples are magnetically ordered for all values

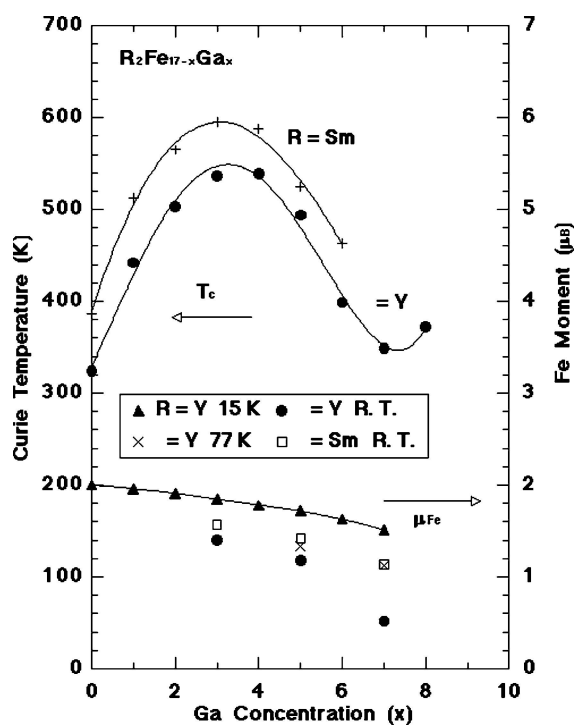


Figure 3 The dependence of the Curie temperature on the Ga concentration for  $Y_2Fe_{17-x}Ga_x$  and  $Sm_2Fe_{17-x}Ga_x$ . The dependence of the value of  $\mu_{Fe}$  on the Ga concentration for  $Y_2Fe_{17-x}Ga_x$  at 15 K obtained from magnetic measurements [4] and at 77 K and room temperature obtained from Mössbauer measurements. The value of  $\mu_{Fe}$  for  $Sm_2Fe_{17-x}Ga_x$  at room temperature obtained from Mössbauer measurements is also shown.

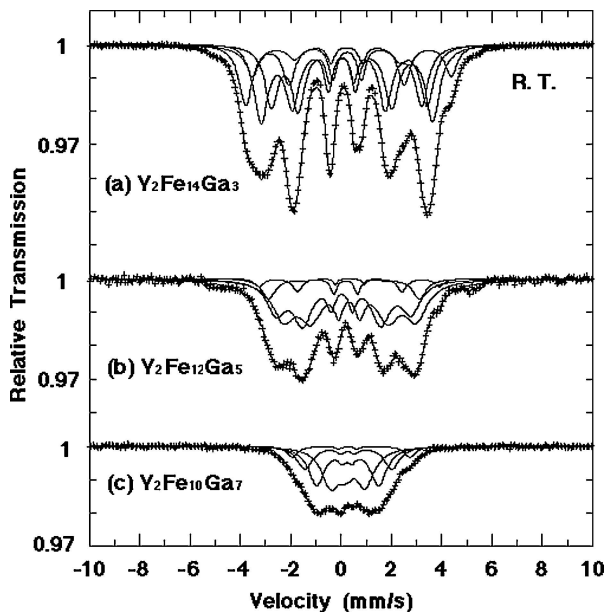


Figure 4 Mössbauer spectra and their fitted curves for (a)  $Y_2Fe_{14}Ga_3$ , (b)  $Y_2Fe_{12}Ga_5$ , (c)  $Y_2Fe_{10}Ga_7$  at room temperature.

of  $x$  and all of them have different subspectra with different magnetic hyperfine fields. The spectra in  $Sm_2Fe_{17-x}Ga_x$  reveal an impurity  $\alpha$ -Fe phase and are fitted as the superposition of five spectra of Fe at the 6c, 9d, 18f and 18h sites and,  $\alpha$ -Fe by the least-squares method. The spectra in  $Y_2Fe_{17-x}Ga_x$  are fitted as the superposition of four spectra of Fe at the 6c, 9d, 18f and 18h sites by the least-squares method.

The concentration dependences of the  $^{57}Fe$  hyperfine fields for  $Y_2Fe_{17-x}Ga_x$  and  $Sm_2Fe_{17-x}Ga_x$  at room temperature are shown in Figs 6 and 7, respectively. The site assignment was done as below. To assign the components of the spectra to the iron site, we had to consider nearest neighbour environments. The 6c site has the largest hyperfine field since it has the largest number of iron nearest neighbors, 13. The 9d and 18f sites have 10 Fe nearest neighbors while the 18h site has the smallest number of iron nearest neighbors, 9. Hence the hyperfine field at the 18f site is larger than that at the 18h site. The hyperfine field at the 9d site can be distinguished from that at the 18h site by its intensities of Mössbauer spectra. Hence we find hyperfine

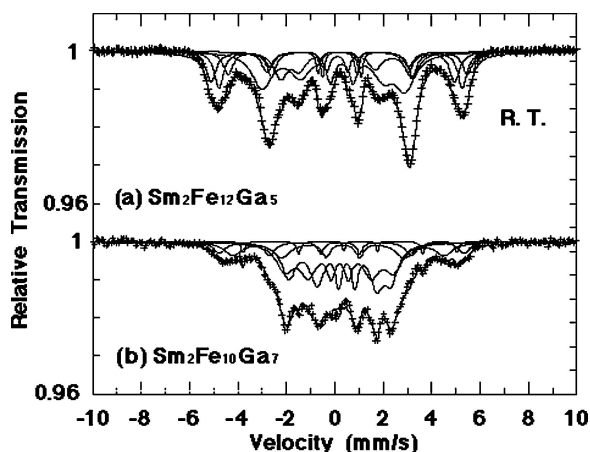


Figure 5 Mössbauer spectra and their fitted curves for (a)  $Sm_2Fe_{12}Ga_5$ , (b)  $Sm_2Fe_{10}Ga_7$  at room temperature.

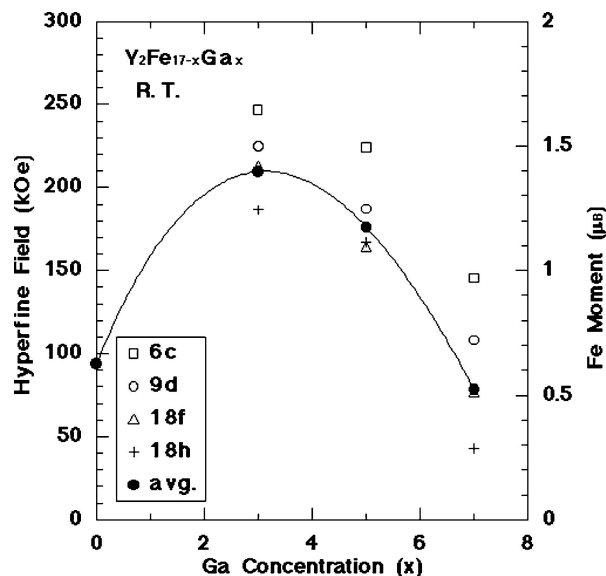


Figure 6 The dependence of the  $^{57}Fe$  hyperfine field and the obtained Fe moment for  $Y_2Fe_{17-x}Ga_x$  on the Ga concentration  $x$  at room temperature. The value of  $Y_2Fe_{17}$  is obtained from ref. [14].

fields for the iron sites that decrease in the order  $6c > 9d > 18f > 18h$ . The site assignment is equal to those in  $Sm_2Fe_{17-x}Al_x$  ( $x = 3$  and  $4$ ) [12] and  $Sm_2Fe_{17-x}Si_x$  for  $0 \leq x \leq 3$  [13].

The value of  $T_C$  for  $Y_2Fe_{17}$  is 324 K and near the room temperature. So the average  $^{57}Fe$  hyperfine field is also small and 94 kOe [14] at room temperature. The average  $^{57}Fe$  hyperfine field increases largely for  $0 \leq x \leq 3$  and decrease for  $3 \leq x \leq 7$  by substituting Fe with Ga, whose change is similar to the change of  $T_C$ . The value of  $T_C$  for  $Sm_2Fe_{17}$  is 387 K and much above the room temperature. So the average  $^{57}Fe$  hyperfine field is large and 221 kOe [14] at room temperature.

The  $^{57}Fe$  hyperfine field decreases with increasing Ga content for  $Y_2Fe_{17-x}Ga_x$  and  $Sm_2Fe_{17-x}Ga_x$ . This decrease results from the decreased magnetic exchange interactions resulting from Ga substitution.

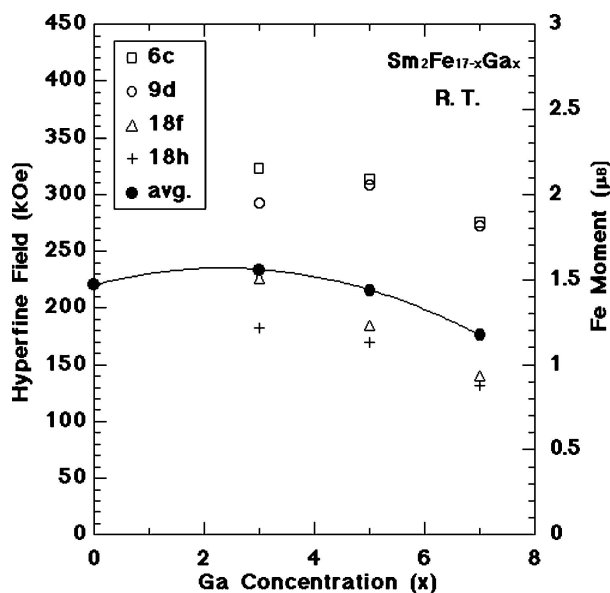


Figure 7 The dependence of the  $^{57}Fe$  hyperfine field and the obtained Fe moment for  $Sm_2Fe_{17-x}Ga_x$  on the Ga concentration  $x$  at room temperature. The value of  $Sm_2Fe_{17}$  is obtained from ref. [14].

The decrease in the average  $^{57}\text{Fe}$  hyperfine field in  $\text{Y}_2\text{Fe}_{17-x}\text{Ga}_x$  and  $\text{Sm}_2\text{Fe}_{17-x}\text{Ga}_x$  for  $3 \leq x \leq 7$  are 131.2 and 57.5 kOe at room temperature, respectively. The reason is that the values of  $T_C$  for  $\text{Y}_2\text{Fe}_{17-x}\text{Ga}_x$  are smaller than those for  $\text{Sm}_2\text{Fe}_{17-x}\text{Ga}_x$  and are near room temperature.

The hyperfine field is, in first approximation, assumed to be proportional to the magnetic moment. If we use the hyperfine coupling constant, 150 kOe/ $\mu_B$ , which has been obtained from the experiments on Y-Fe systems [15], we obtain the Fe moment at each site in  $\text{Y}_2\text{Fe}_{17-x}\text{Ga}_x$  and  $\text{Sm}_2\text{Fe}_{17-x}\text{Ga}_x$  at room temperature as shown in Figs 6 and 7, respectively. The average values of  $\mu_{\text{Fe}}$  obtained from Mössbauer measurements in  $\text{Y}_2\text{Fe}_{17-x}\text{Ga}_x$  and  $\text{Sm}_2\text{Fe}_{17-x}\text{Ga}_x$  are shown with those obtained from magnetic measurements at 15 K [4] in Fig. 3. In  $\text{Y}_2\text{Fe}_{17-x}\text{Ga}_x$  the values of  $\mu_{\text{Fe}}$  decrease with increasing temperature.

The concentration dependences of the average isomer shift at room temperature for  $\text{Y}_2\text{Fe}_{17-x}\text{Ga}_x$  and  $\text{Sm}_2\text{Fe}_{17-x}\text{Ga}_x$  are shown in Fig. 8. The assignment of the hyperfine parameter set of a given sextet to its crystallographic site obeys the relationship between the isomer shift and the Wigner-Seitz cell (WSC) volumes: the larger the WSC volume the larger the isomer shift [16]. For  $\text{Sm}_2\text{Fe}_{17-x}\text{Si}_x$  ( $x = 0, 1, 2$ ) [17] it appears clearly that whatever  $x$ , the WSC volume of the 6c site is always the largest and WSC volume of the 9d site is the smallest. The WSC volumes of the 18f and 18h sites are medium and close together. The site assignment for  $\text{Y}_2\text{Fe}_{14}\text{Ga}_3$  follows the above explanations. Upon Ga substitution of  $\text{Y}_2\text{Fe}_{17-x}\text{Ga}_x$ , the average isomer shift,  $\delta$ , increases from 0.17 ( $x = 3$ ) to 0.30 mm/s ( $x = 7$ ).

The values of  $\delta$  for  $\text{Y}_2\text{Fe}_{17-x}\text{Ga}_x$  at room temperature are positive and the magnitudes of  $\delta$  increase with increasing Ga content as shown in Fig. 8. The parameters

for the linear fitting are given by the equation

$$\delta(\text{mm/s}) = 0.04x - 0.03. \quad (1)$$

The volume effect on the iron isomer shift,  $\Delta\delta/\Delta(\ln V)$ , where  $V$  is the unit cell volume, for  $\text{Y}_2\text{Fe}_{17-x}\text{Ga}_x$  was 4.81 mm/s compared to 1.13 mm/s for  $\alpha\text{-Fe}$  [18] and 1.5–2.3 mm/s for  $\text{R}_2\text{Fe}_{17}$  and  $\text{R}_2\text{Fe}_{17}\text{N}_{3-\delta}$  at 15 K [15]. The present value is larger than those values due to the smaller change in the cell volume. A plot of  $\delta$  versus the unit cell volume reveals a perfectly linear correlation where

$$(\text{mm/s}) = 5.9 \times 10^{-3}((\text{mm/s})/\text{\AA})V - 4.64. \quad (2)$$

Thus, the variation in  $\delta$  with  $x$  shown in Fig. 8 is directly related to the expansion of the unit cell volume upon Ga. Hence, the increase of  $\delta$  implies a decrease in the s-electron density at the nucleus which can be attributed to the expansion of the unit cell volume.

The similar tendency of the isomer shifts for  $\text{Sm}_2\text{Fe}_{17-x}\text{Ga}_x$  is observed. The values of  $\delta$  for  $\text{Sm}_2\text{Fe}_{17-x}\text{Ga}_x$  at room temperature are positive and the magnitude of  $\delta$  increase with increasing Ga content as shown in Fig. 8. The parameters for the linear fitting are given by the equation

$$\delta(\text{mm/s}) = 0.04x + 0.04. \quad (3)$$

$\Delta\delta/\Delta(\ln V)$ , where  $V$  is the unit cell volume, for  $\text{Sm}_2\text{Fe}_{17-x}\text{Ga}_x$  was 4.60 mm/s. A plot of  $\delta$  versus the unit cell volume reveals a perfectly linear correlation where

$$\delta(\text{mm/s}) = 5.72 \times 10^{-3}((\text{mm/s})/\text{\AA}^3)V - 4.49. \quad (4)$$

The change of  $\delta$  for  $\text{Y}_2\text{Fe}_{17-x}\text{Ga}_x$  is similar to that for  $\text{Sm}_2\text{Fe}_{17-x}\text{Ga}_x$ . For  $\text{SmFe}_{7-x}\text{B}_x$  with rhombohedral  $\text{Th}_2\text{Zn}_{17}$  type phase at room temperature in our previous paper [19],

$$\delta(\text{mm/s}) = 9.25 \times 10^{-3}((\text{mm/s})/\text{\AA})V - 7.27 \quad (5)$$

is obtained. The change of  $\delta$  for  $\text{SmFe}_{7-x}\text{B}_x$  with increasing the unit cell volume is larger than that for  $\text{Sm}_2\text{Fe}_{17-x}\text{Ga}_x$ .

The values of the quadrupole splittings, QS, for  $\text{Y}_2\text{Fe}_{17-x}\text{Ga}_x$  are small and lie between  $-0.5$  and  $0.2$  mm/s at room temperature. The change in the values of QS at the 9d site is large. The values of QS for  $\text{Sm}_2\text{Fe}_{17-x}\text{Ga}_x$  lie between  $-0.5$  and  $0.1$  mm/s at room temperature. The sign of the average values of QS is positive for  $\text{Y}_2\text{Fe}_{17-x}\text{Ga}_x$  and negative for  $\text{Sm}_2\text{Fe}_{17-x}\text{Ga}_x$ .

#### 4. Conclusions

The magnetic properties of  $\text{Y}_2\text{Fe}_{17-x}\text{Ga}_x$  and  $\text{Sm}_2\text{Fe}_{17-x}\text{Ga}_x$  for  $3 \leq x \leq 7$  have been investigated using the  $^{57}\text{Fe}$  Mössbauer spectroscopy at room temperature. These compounds have the rhombohedral  $\text{Th}_2\text{Zn}_{17}$  structure. X-ray diffraction analyses of

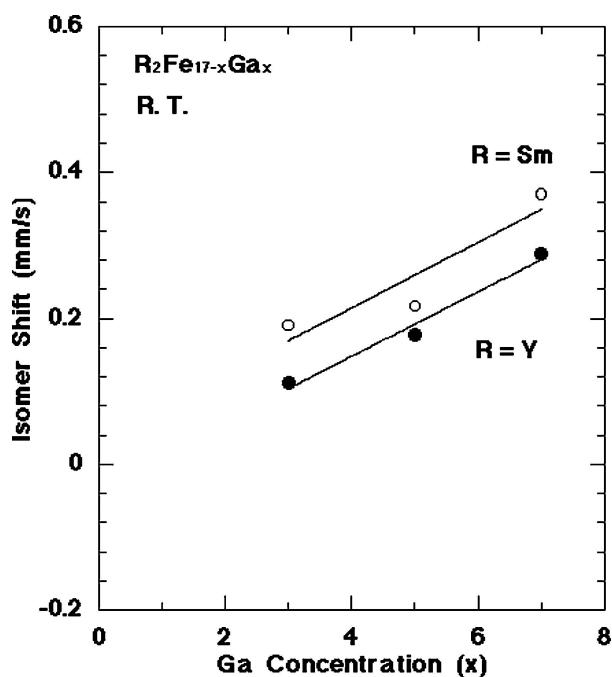


Figure 8 The dependence of the average isomer shift for  $\text{Y}_2\text{Fe}_{17-x}\text{Ga}_x$  and  $\text{Sm}_2\text{Fe}_{17-x}\text{Ga}_x$  on the Ga concentration  $x$  at room temperature.

aligned powders show that the easy direction of magnetization is parallel to the c-axis in  $Y_2Fe_{10}Ga_7$  and  $Sm_2Fe_{14}Ga_3$  and is perpendicular to the c-axis in  $Y_2Fe_{14}Ga_3$ ,  $Y_2Fe_{12}Ga_5$ ,  $Sm_2Fe_{12}Ga_5$  and  $Sm_2Fe_{10}Ga_7$ .

Mössbauer studies indicate that all the samples studied are ferromagnetically ordered. The  $^{57}Fe$  hyperfine field decreases for  $3 \leq x \leq 7$  with increasing Ga content. This decrease results from the decreased magnetic exchange interactions resulting from Ga substitution. The average isomer shift,  $\delta$ , for  $Y_2Fe_{17-x}Ga_x$  and  $Sm_2Fe_{17-x}Ga_x$  at room temperature is positive and the magnitude of  $\delta$  increases with increasing Ga content, which implies a decrease in the s-electron density at the nucleus that can be attributed to the expansion of the unit cell volume.

## References

1. B. G. SHEN, Z. H. CHENG, B. LIANG, H. Q. GUO, J. X. ZHANG, H. Y. GONG, F. W. WANG, Q. W. YAN and W. S. ZHAN, *Appl. Phys. Lett.* **67** (1995) 1621.
2. Z. WANG and R. A. DUNLAP, *J. Phys.: Cond. Matt* **5** (1993) 2407.
3. B. G. SHEN, B. LIANG, F. W. WANG, Z. H. CHENG, H. Y. GONG, S. Y. ZHANG and J. X. ZHANG, *J. Appl. Phys.* **77** (1995) 2637.
4. B. G. SHEN, Z. H. CHENG, H. Y. GONG, B. LIANG, Q. W. YAN, F. W. WANG, J. X. ZHANG, S. Y. ZHANG and H. Q. GUO, *J. Alloys Compd.* **226** (1995) 51.
5. B. G. SHEN, F. W. WANG, L. S. KONG and L. CAO, *J. Phys.: Cond. Matt* **5** (1993) L685.
6. Z. H. CHENG, B. G. SHEN, B. LIANG, J. X. ZHANG, F. W. WANG, S. Y. ZHANG, J. G. ZHAO and W. S. ZHAN, *J. Appl. Phys.* **78** (1995) 1385.
7. Y. HAO, *J. Magn. Magn. Mater.* **214** (2000) 119.
8. F. WANG, B. G. SHEN, P. ZHNG, Z. H. CHENG, J. ZHANG, H. GONG, B. LIANG, X. SUN and Q. YAN, *J. Appl. Phys.* **83** (1998) 3250.
9. B. G. SHEN, Z. H. CHENG, F. W. WANG, Q. W. TAN, H. TANG, B. LIANG, S. Y. ZHANG, F. R. DE BOER, K. H. J. BUSCHOW and S. RIDWAN, *ibid.* **83** (1998) 5945.
10. F. MARUYAMA, unpublished.
11. Q. W. YAN, P. L. ZHANG, X. D. SHEN, B. G. CHEN, Z. H. CHEG, C. GOU, D. F. CHEN, RIDWAN, MUMJILAH, GUNAWAN and MARSONGKOHADI, *J. Phys.: Cond. Matt* **8** (1996) 1485.
12. G. J. LONG, O. A. PRINGLE, P. C. EZEKWENNA, S. R. MISHRA, D. HAUTOT and F. GRANDJEAN, *J. Magn. Magn. Mater.* **186** (1998) 10.
13. Z. W. LI, X. Z. ZHOU and A. H. MORRISH, *Phys. Rev.* **B51** (1995) 2891.
14. B. P. HU, H. S. LI, H. SUN and J. M. D. COEY, *J. Phys.: Cond. Matt* **3** (1991) 3983.
15. Z. W. LI, X. Z. ZHOU and A. H. MORRISH, *J. Phys.: Cond. Matt* **4** (1992) 10409.
16. C. D. MARIADASSOU, L. BESSAIS, A. NANDRA and E. BURZO, *Phys. Rev.* **B68** (2003) 024406.
17. C. D. MARIADASSOU, L. BESSAIS, A. NANDRA, J. M. GRENECHE and E. BURZO, *ibid.* **B65** (2001) 014419.
18. D. L. WILLIAMSON, in "Mössbauer Isomer Shifts", edited by G. K. Shenoy and F. E. Wagner (North-Holland, Amsterdam, 1978) p. 317.
19. F. MARUYAMA and H. NAGAI, *J. Alloys Compd.* **393** (2005) 61.

Received 11 December 2004  
and accepted 19 April 2005